AIP | The Journal of Chemical Physics

Non-Markovian dynamics of single- and two-qubit systems interacting with Gaussian and non-Gaussian fluctuating transverse environments

Matteo A. C. Rossi and Matteo G. A. Paris

Citation: The Journal of Chemical Physics **144**, 024113 (2016); doi: 10.1063/1.4939733
View online: http://dx.doi.org/10.1063/1.4939733
View Table of Contents: http://scitation.aip.org/content/aip/journal/jcp/144/2?ver=pdfcov
Published by the AIP Publishing

Non-Markovian dynamics of single- and two-qubit systems interacting with Gaussian and non-Gaussian fluctuating transverse environments

Matteo A. C. Rossi[1,a] and Matteo G. A. Paris[1,2,b]
[1]*Quantum Technology Lab, Dipartimento di Fisica, Università degli Studi di Milano, 20133 Milano, Italy*
[2]*CNISM, Unità Milano Statale, I-20133 Milano, Italy*

(Received 20 October 2015; accepted 28 December 2015; published online 12 January 2016)

We address the interaction of single- and two-qubit systems with an external *transverse* fluctuating field and analyze in detail the dynamical decoherence induced by Gaussian noise and random telegraph noise (RTN). Upon exploiting the exact RTN solution of the time-dependent von Neumann equation, we analyze in detail the behavior of quantum correlations and prove the non-Markovianity of the dynamical map in the full parameter range, i.e., for either fast or slow noise. The dynamics induced by Gaussian noise is studied numerically and compared to the RTN solution, showing the existence of (state dependent) regions of the parameter space where the two noises lead to very similar dynamics. We show that the effects of RTN noise and of Gaussian noise are different, i.e., the spectrum alone is not enough to summarize the noise effects, but the dynamics under the effect of one kind of noise may be *simulated* with high fidelity by the other one. © *2016 AIP Publishing LLC*. [http://dx.doi.org/10.1063/1.4939733]

I. INTRODUCTION

The unavoidable interaction of a quantum system with its environment generally causes decoherence and a loss of quantumness, thus posing a threat to quantum information processing. A deep understanding of the decoherence mechanisms in quantum systems, together with the capability to engineer the environment, is thus a very important step toward the development of quantum technologies.

In general, a quantum system interacts with a complex environment that should be described quantum-mechanically. This is often challenging or even unfeasible in practice, unless one recurs to perturbative approximations[1,2] or to approximations that reduce the description of the environment to a few degrees of freedom.[3–6] In many situations, the environment may be conveniently represented as a collection of fluctuators, such that it can be described as a classical stochastic field such as, for instance, a Gaussian process or random telegraph noise (RTN).[7–10] A relevant example is that of charge noise in superconducting qubits or quantum dots, which may be conveniently modeled by a classical field as far as the charge fluctuators couple more strongly to their own environment than to the qubit.[11–13] More generally, addressing RTN is relevant since solid state or superconducting devices may often be described by models in which noise is due to a collection of bistable fluctuators, e.g., resulting in a $1/f$ spectrum, f being the frequency.[14]

It is a subject of current research[15–19] whether the interaction with quantum environments may be effectively described by a classical stochastic field. So far, full equivalence has been shown in Ref. 18 for single-qubit dephasing, with an explicit construction of the probability distribution required for the classical stochastic process to describe the quantum environment. General arguments valid for RTN noise have been also discussed.[20] A stochastic process approach may be also used to decouple the dynamics of the system from that of its environment, with the two separated systems evolving in common classical random fields.[21]

Among the different classes of open quantum systems, a large attention has been put to qubit systems subject to environmental noise inducing a dephasing dynamics,[10,22] i.e., noise with typical frequencies that are smaller than the characteristic frequencies of the quantum system. In these situations, the energy of the system is not altered by the interaction and only the coherences are affected. For the dephasing model, analytic solutions have been found for Gaussian noise[23] and RTN,[12,24,25] and numerically for colored noise.[26] A number of interesting features have been discovered and studied, such as entanglement sudden death (ESD)[23] and quantum discord freezing.[27] Moreover, the non-Markovianity of the dynamics has been addressed,[28] and the use of qubits as probes for the spectral properties of the environment has been proposed.[29–32] Recently, the role of entanglement in improving the estimation of dephasing environments has been recognized,[33] thus making of interest the study of decoherence in more general environments.[34,35]

The dephasing Hamiltonian for a single qubit under the effect of an external field is $\mathcal{H}(t) = \omega\sigma_z + \lambda\, B(t)\,\sigma_z$, where ω is the energy between the energy levels, λ is a coupling constant, and $B(t)$ is a stochastic process that models the external noise (we set $\hbar = 1$). This is usually referred to as *longitudinal noise*,[36,37] the direction of the external driving being parallel to the qubit axis in the spin space. From a physical point of view, dephasing processes correspond to transitions where the environment changes its state, while the qubit system remains unchanged. Since almost no energy is exchanged, dephasing is relevant when the low energy part

[a]Electronic mail: matteo.rossi@unimi.it. URL: http://users.unimi.it/aqm.
[b]Electronic mail: matteo.paris@fisica.unimi.it. URL: http://users.unimi.it/aqm.

of environment spectrum is dominant. In turn, in a dephasing model, the populations of the system are constant.

On the other hand, if the typical frequencies of the environment are close to the characteristic frequency of the qubit, the interaction induces transitions between the energy levels and the pure dephasing model is inadequate to describe the dynamics. The Hamiltonian must include a transverse interaction describing the damping and hopping (relaxation and excitation) mechanisms induced by the environment[38–40] and, in general, may be written as

$$\mathcal{H}(t) = \omega\sigma_z + B(t)\,\boldsymbol{\lambda}\cdot\boldsymbol{\sigma}. \tag{1}$$

In this paper, we analyze in detail the case in which the interaction is purely transverse, i.e., when $\lambda_z = 0$. The topic is relevant for any system where excitation and relaxation processes take place, e.g., for energy relaxation,[41,42] or motional averaging[43] in superconducting qubits, charge noise in semiconductor qubits,[44] and spin-$\frac{1}{2}$ particles immersed in a generic magnetic field.[45,46]

We address the dynamics of single- and two-qubit systems under the effect of RTN, a non-Gaussian kind of noise, and provide an exact analytic description of the resulting decoherence process. We also address numerically the dynamics induced by Gaussian noise. We analyze the evolution of quantum correlations, evaluate the non-Markovianity of the dynamical map, and compare the effects of the two kinds of noise, looking for features that depend on the sole spectrum of the noise and not on higher-order correlations.

Our results show that the effects of non-Gaussian noise cannot be trivially mapped to that of Gaussian noise and vice versa, i.e., the spectrum alone is not enough to summarize the noise effects: the different statistics of the two noises under study affect the dynamics of the system. On the other hand, the dynamics under the effect of one kind of noise may be effectively simulated, i.e., with high quantum fidelity, by the other one with a suitable choice of the noise parameters. This choice, however, does depend on the initial state of the system and thus no general relation between the parameters of the two noises may be established.

Besides, we have identified, for both kinds of noise, two different working regimes. In the first one, when the spectral width of the noise γ is small, compared to the coupling energy, quantum correlations oscillate heavily and there are sudden deaths and rebirths of entanglement. This is the so-called slow-noise or strong-coupling regime.[36] The frequency of oscillations depends on ω and is doubled if the two qubits are affected by a common environment. In the second regime (fast-noise or weak-coupling regime) the correlations decay to zero, with sudden death of entanglement and with oscillations. The time constant of the decay is roughly inversely proportional to γ, i.e., the decay is slower for very fast noise. The different features of the dynamics, however, cannot be linked to a transition in the structure of the dynamical map, which is non-Markovian in the full parameter range, i.e., for either fast or slow noise.

The structure of the paper is as follows: in Section II, we present the model and introduce the measures of quantum correlations and non-Markovianity. In Section III, we present the solution of the dynamics of the system, whereas in Section IV, we study the evolution of quantum correlations and compare the dynamics induced by the two kinds of noise. In Section V, we discuss the non-Markovianity of the dynamical maps, whereas Section VI, closes the paper with some concluding remarks.

II. THE MODEL

We consider a qubit characterized by the energy splitting ω, and affected by a transverse noise. The Hamiltonian is

$$\mathcal{H}(t) = \omega\sigma_z + \lambda B(t)\sigma_x, \tag{2}$$

where we assume without loss of generality that the noise acts in the x direction. The evolution operator for the Hamiltonian in Eq. (2), for a given realization of the stochastic process $B(t)$, is

$$U(t) = \mathcal{T}\exp\left(-i\int_0^t \mathcal{H}(t')dt'\right), \tag{3}$$

where $\mathcal{T}$ is the time-ordering operator, which is required because the Hamiltonian does not commute with itself at different times. If the qubit is initially prepared in the state described by the density matrix ρ_0, the density matrix at the time t is

$$\rho(t) = \left\langle U(t)\rho_0 U(t)^\dagger \right\rangle, \tag{4}$$

where $\langle\cdot\rangle$ denotes the average over all possible realizations of the stochastic process $B(t)$. Equation (4) describes a convex combination of unitary operators, which itself provides the Kraus decomposition of the corresponding CPT map.

We are also going to consider a system of two identical, non-interacting qubits each interacting with a noisy environment, in order to study the evolution of quantum correlations between the qubits. The two-qubit Hamiltonian reads

$$\mathcal{H}(t) = \mathcal{H}_1(t)\otimes\mathbb{I}_2 + \mathbb{I}_1\otimes\mathcal{H}_2(t), \tag{5}$$

where $\mathcal{H}_i(t)$ have the form of Eq. (2) and the $B_i(t)$ may be correlated (if the two qubits interact with a common environment) or completely uncorrelated (in the case in which the two qubits are affected by independent environments, IE). For simplicity, we will consider $B_1(t) = B_2(t)$ in the common environment (CE) case.

A Gaussian process is fully characterized by its second order statistics, i.e., by its mean μ and its autocorrelation function K, in formula

$$\mu(t) = \langle B(t)\rangle, \tag{6}$$

$$K(t,t') = \langle B(t)B(t')\rangle. \tag{7}$$

In this work, we employ the Ornstein-Uhlenbeck (OU) process[47–49] as a paradigmatic stationary stochastic process with finite-time correlations. We set $\mu(t) \equiv 0$ and assume the following autocorrelation function:

$$K_{\mathrm{OU}}(t-t') = e^{-2\gamma|t-t'|}, \tag{8}$$

which corresponds to a Lorentzian spectrum

$$S(\omega) = \frac{4\gamma}{4\gamma^2 + \omega^2}, \tag{9}$$

with spectral width 2γ. For $\gamma \to \infty$, $K(t-t') \sim \delta(t-t')$, i.e., the OU process reduces to white noise.

RTN noise is produced by bistable fluctuators, i.e., systems where a quantity flips between two values with a certain switching rate, such as a resistance switching between two discrete values, charges jumping between two different locations, or electrons that flip their spin. In order to describe classical environment inducing RTN, the quantity $B(t)$ in Eq. (2) should flip randomly between the values ± 1 with a given switching rate γ. This kind of noise is also characterized by an exponentially decaying autocorrelation function

$$K_{\mathrm{RTN}}(t-t') = e^{-2\gamma|t-t'|} \tag{10}$$

and by a Lorentzian spectrum $S(\omega)$, Eq. (9), i.e., the OU and RTN processes have exactly the same autocorrelation function. The latter, however, being a non-Gaussian process, cannot be fully described by means of its first and second moments.

For either kind of noise, the model exhibits a natural scaling property in terms of the coupling, which may be exploited in order to work with dimensionless quantities. Indeed, we rescale all the quantities in terms of the coupling λ by performing the following substitutions:

$$t \to \lambda t, \quad \gamma \to \gamma/\lambda, \quad \omega \to \omega/\lambda.$$

The Hamiltonian, Eq. (2), now reads

$$\mathcal{H}(t) = \omega\sigma_z + B(t)\sigma_x. \tag{11}$$

A. Quantum correlations

In the following, we will study the dynamics of quantum correlations by evaluating negativity[50] as a measure of entanglement and using entropy[51] to define quantum discord. Negativity is defined as

$$\mathcal{E} = 2\left|\sum_i \lambda_i^-\right|, \tag{12}$$

where λ_i^- are the negative eigenvalues of the partial transpose of the density matrix with respect to either of the qubits. We remark that the negativity of the partial transpose is necessary and sufficient for two-qubit systems to be entangled.

Quantum discord is defined as the difference between the total correlations and the classical correlations between the two subsystems,

$$\mathcal{D} = \mathcal{I} - C. \tag{13}$$

Total correlations are given by the quantum mutual information $\mathcal{I} = S(\rho_A) + S(\rho_B) - S(\rho)$, where S is the von Neumann entropy, and ρ_A and ρ_B are the reduced density matrices of the two subsystems. Classical correlations, induced by a measurement on one of the two subsystems, are given by $C = \max_{\{B_k\}}[S(\rho_A) - S(\rho|\{B_k\})]$, where $S(\rho|\{B_k\})$ is the conditional entropy of the state of the two-qubit system with respect to the outcome of the measurement $\{B_k\}$ on system B, and the maximization is carried over all possible projective measurements.

The evaluation of quantum discord is in general a difficult task, as it involves an optimization procedure. For two-qubit systems, an analytic result was found by Luo[52] for a subset of the state space, i.e., for those states that have maximally mixed marginals. As we are going to show below, if the initial state of the system belongs to this subset, the dynamics induced by transverse noise is limited to this subset, so we will employ Luo's formula in the following.

B. Non-Markovianity measures

The concept of non-Markovianity for quantum dynamical maps is related to the concept of divisibility, i.e., if $\Phi(t_2,t_0)$ is the operator describing the quantum map from time t_0 to t_2, the map is divisible if it is completely positive (CP) and

$$\Phi(t_2,t_0) = \Phi(t_2,t_1)\Phi(t_1,t_0), \tag{14}$$

for every intermediate time $t_0 < t_1 < t_2$. We characterize the non-Markovianity of the quantum map by considering two measures: the entanglement-based Rivas-Huelga-Plenio (RHP) measure[53] and the Breuer-Laine-Piilo (BLP) measure,[54] based on the time evolution of the trace distance. These two measures define sufficient conditions for the dynamical map to be non-Markovian. Here, we briefly review the two measures.

1. RHP measure

We consider the quantum system of interest, S, and an identical ancillary system A. We prepare the two system in the maximally entangled state

$$|\psi\rangle = \frac{1}{\sqrt{N}}\sum_{n=1}^{N} |n\rangle_S|n\rangle_A, \tag{15}$$

where $|n\rangle$ are the vectors of a basis of the Hilbert space of the system. We now let the system S interact with the environment, while the ancilla A is left untouched, and evaluate the entanglement of the state $|\psi(t)\rangle$. Since any entanglement measure is a monotone under local CP maps, any increase of an entanglement measure with time denotes that the dynamical map fails to be divisible, i.e., that it is non-Markovian. The RHP is defined quantitatively as

$$\mathcal{N}_{\mathrm{RHP}} = \int_{t_0}^{t_f} \left|\frac{d\mathcal{E}(t)}{dt}\right|, \tag{16}$$

where $\mathcal{E}(t)$ is any entanglement measure (in our case, the negativity). In fact, Ref. 53 introduces another measure that is a necessary and sufficient condition for the non-Markovianity of the quantum map, based on the Choi-Jamiolkowski isomorphism. However, to compute this measure, one needs to know the structural form of the dynamical map between any two time instants, which is not the case for our processes.

2. BLP measure

The BLP measure is based on the fact that the trace distance, $D(\rho_1,\rho_2) = \frac{1}{2}\mathrm{Tr}\left[\sqrt{(\rho_1-\rho_2)^2}\right]$, is contractive for CP

maps, so if the quantum map is divisible, then for any pair of initial states of the system the trace distance between the evolved states is a monotonically decreasing function of time. If in a certain time interval the trace distance increases, we can say that the CP map under investigation is non-Markovian, because the map fails to be divisible in that interval of time. The BLP measure is computed by integrating with respect to time the positive part of the time derivative of the trace distance and then optimizing the result over all possible pairs of states:

$$\mathcal{N}_{\mathrm{BLP}} = \max_{(\rho_1,\rho_2)} \int_{t_0}^{t_f} \left[\frac{d}{dt} D(t,\rho_1,\rho_2)\right]_+ dt. \tag{17}$$

Calculating the BLP measure may be challenging in general, as the optimization over all possible pairs of states is required. For qubits however, the optimization can be restricted to the surface of the Bloch sphere,[55] leaving only the polar and azimuth angles as parameters to optimize over.

III. SOLUTION OF THE DYNAMICS

In order to obtain a solution for $\rho(t)$ in Eq. (4), one should at first find an explicit expression for the evolution operator $U(t)$ in Eq. (3) and then calculate the expected value over all possible realizations of the stochastic process.

A. Gaussian noise: Numerical simulation

For Gaussian noise an explicit expression for $U(t)$ is only possible by means of approximations such as the Dyson series or the Magnus expansion,[56] which are valid in a neighborhood of the initial time. A cumulant expansion has been also introduced and discussed in the single-qubit case.[46,57–59] The lack of an exact analytic solution is due to the fact that the time-dependent Hamiltonian does not commute with itself at different times and we cannot find an explicit expression for the time-ordered exponential. An analytic result can be obtained in the approximation of a quasi-static external field, i.e., when the stochastic process is weakly dependent on time and the two-time commutator for the Hamiltonian is negligible.[49]

The dynamics of the system may be studied numerically using different approaches.[45,46] We proceed in a straightforward way by numerical evaluation of the unitary propagator upon discretizing the time interval $[0,t]$ in n steps of length Δt. Δt should be small enough for $H(t)$ to be approximately constant in the time interval. The evolution operator from t_i to t_{i+1} for a specific realization of the process $B(t)$ reads $U_{t_i,t_{i+1}} \simeq \exp[-iH(t_i)\Delta t]$. The density operator of the qubit is then given by

$$\rho(t) \simeq \left\langle U_{t_{n-1},t_n} \cdots U_{t_1,t_2} \rho_0 U^\dagger_{t_1,t_2} \cdots U^\dagger_{t_{n-1},t_n} \right\rangle. \tag{18}$$

The expected value is obtained from a sufficiently large number N of randomly generated realizations of the noise. This method converges as N increases. We have checked that the standard deviation decreases as $1/\sqrt{N}$. Typical values for N are of the order of 10^5 to 10^6, with the maximum relative error on an element of the density matrix of the order of $10^{-3}/10^{-4}$ after 100 evolution steps.

B. Analytic solution for the RTN

Analytic solutions for a qubit interacting with RTN with an arbitrary direction are known.[60–62] By following Ref. 60, we consider the time evolution of the Bloch vector $\mathbf{n}(t)$, which can be written by means of a transfer matrix T applied to the initial Bloch vector $\mathbf{n}(0)$ as

$$\mathbf{n}(t) = T\mathbf{n}(0) = \left\langle T_{s_n} \cdots T_{s_1} \right\rangle \mathbf{n}(0), \tag{19}$$

where T_{s_i} is the 3×3 transfer matrix from the time instant t_i to time t_{i+1}, when the fluctuator is in the state $s_i = \pm 1$. T_{s_i} has the following expression:

$$T_{s_i} = \exp[-2i\Delta t(\omega L_z + s_i L_x)], \tag{20}$$

where L_i are the generators of $SO(3)$, $(L_i)_{jk} = -i\epsilon_{ijk}$, satisfying the commutation relations $[L_i, L_j] = i\sum_k \epsilon_{ijk} L_k$. The transfer matrix for a n-step evolution may be written as

$$T = \langle x_f | \Gamma^n | i_f \rangle, \tag{21}$$

where $|x_f\rangle = \frac{1}{\sqrt{2}}(|+\rangle + |-\rangle)$, $|i_f\rangle$ is the initial distribution of the states of the fluctuator (in our case the two states are equiprobable, $|i_f\rangle = \frac{1}{\sqrt{2}}(|+\rangle + |-\rangle)$) and Γ is the 6×6 matrix

$$\begin{aligned}\Gamma = {} & [(1-\gamma\Delta t)\mathbb{I}_2 + \gamma\Delta t\sigma_1] \otimes \mathbb{I}_3 \\ & \times \exp[-2i\Delta t(\omega L_z \mathbb{I}_2 + L_x \sigma_3)],\end{aligned} \tag{22}$$

where $\times$ denotes a product between 6×6 matrices. The partial inner product in Eq. (21) is done in the two degrees of freedom of the fluctuator and the result is a 3×3 matrix.

In the continuous limit $\Delta t \to 0$, Eq. (21) becomes

$$T = \langle x_f | \exp(-tP) | i_f \rangle, \tag{23}$$

where

$$P = (\gamma - \gamma\sigma_1) \otimes \mathbb{I}_3 - 2i\omega \mathbb{I}_2 \otimes L_z - 2i\sigma_3 \otimes L_x. \tag{24}$$

The problem is now cast into the diagonalization of the 6×6 matrix P. The eigenvalues μ_i, η_i, $i = 1,2,3$, of P satisfy the two equations

$$\mu^3 + 2\gamma\mu^2 + 4(1+\omega^2)\mu + 8\omega^2\gamma = 0, \tag{25}$$

$$\eta^3 + 4\gamma\eta^2 + 4(1+\gamma^2+\omega^2)\eta + 8\gamma = 0. \tag{26}$$

We notice that we can linearly transform one equation into the other by substituting $\nu = -\mu - 2\gamma$. The inverse of the real parts of these eigenvalues gives the decay rate of the Bloch vector components, while the inverse of the imaginary parts gives the periods of oscillations. The matrix elements of T are reported in Appendix for reference.

In the limiting cases of γ much greater or smaller than the other two parameters, we are able to obtain analytic expressions for the eigenvalues. When $\gamma \gg \omega$, i.e., we are in the fast-noise regime, we find that the greatest decay time is

$$T = \gamma, \tag{27}$$

while the oscillation frequency is ω, independently of γ. In the opposite limiting case, $\gamma \ll \omega$, we find that the longest

decay time is

$$T = \begin{cases} \gamma^{-1}(1+\omega^2) & \text{if } \omega > 1/\sqrt{2} \\ \frac{1}{2}\gamma^{-1}(1+1/\omega^2) & \text{if } \omega < 1/\sqrt{2} \end{cases}, \tag{28}$$

while the oscillation frequency is instead $\sqrt{1+\omega^2}$. In the intermediate region, by studying the discriminant of Eq. (25), we find that for $\omega < 1/(2\sqrt{2})$ there is a region of values of γ for which the eigenvalues are all real, i.e., there are no oscillations. This region, shown in Fig. 1, is bounded from below and above, respectively, by the two positive solutions $\gamma_{1,2}$ of

$$4\omega^2\gamma^4 + \left(8\omega^4 - 20\omega^2 - 1\right)\gamma^2 + 4\left(\omega^2+1\right)^3 = 0. \tag{29}$$

For $\omega \to 0$, $\gamma_1 \to 2$ and $\gamma_2 \to \infty$, so we recover the transition between fast and slow RTN that is visible in the dephasing case.[7,63] In fact, by letting $\omega \to 0$ we are implying that the energy gap between the levels of the qubit is far away from the typical frequencies of the noise. A sharp transition between the two regimes is not visible by looking at the time evolution of the Bloch components because the imaginary components tend to zero as the parameters get close to the region, and thus the period of oscillation becomes much larger than the characteristic decay time.

In Fig. 2 we show the dynamical trajectories in the Bloch sphere for two different initial preparations. The asymptotic state is the maximally mixed state, with Bloch vector $(0,0,0)$.

C. Transfer matrix for the two-qubit case

The transfer matrix method can be generalized to the two-qubit dynamics for both the relevant, and opposed, scenarios of independent environments and of a common environment. The generalization of the Bloch vector to the two-qubit case is a 15-component vector defined as follows:

$$\mathbf{n}_2 = (\mathbf{a}, \mathbf{b}, c_{11}, c_{12}, c_{13}, c_{21}, c_{22}, c_{23}, c_{31}, c_{32}, c_{33}), \tag{30}$$

where $\mathbf{a} = (a_1, a_2, a_3)$, $\mathbf{b} = (b_1, b_2, b_3)$, and c_{ij} are the elements of a 3×3 matrix C. The two-qubit density matrix may be

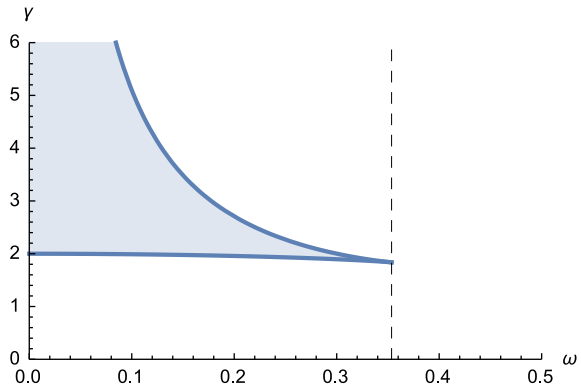

FIG. 1. Shaded region: values of the parameters ω and γ for which the eigenvalues of the operator P, i.e., the solutions of Eqs. (25) and (26) are all real, that is, there are no oscillating terms in the transfer matrix. The region is bounded by the solutions of Eq. (29), which meet at the threshold value $\omega = (2\sqrt{2})^{-1}$, highlighted by the vertical dashed line. For $\omega \to 0$, we recover the dephasing case, with a transition between the two regimes at $\gamma = 2$.

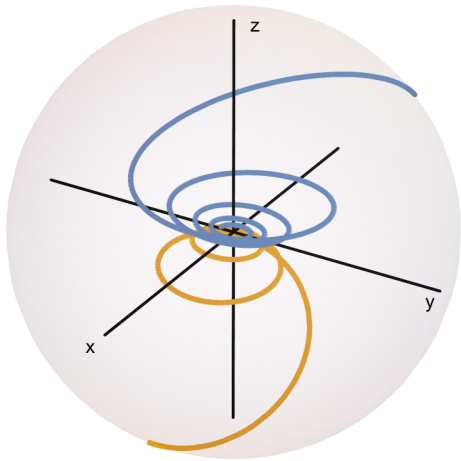

FIG. 2. Dynamical trajectories in the Bloch sphere for a single qubit affected by RTN with $\gamma = 1/2$ and $\omega = 1$ and for different initial preparations. The initial state is represented by the Bloch vector $\frac{1}{\sqrt{3}}(-1,1,1)$ for the blue trajectory and by $\frac{1}{\sqrt{2}}(1,0,-1)$ for the orange trajectory. The asymptotic state is the maximally mixed state, with Bloch vector $(0,0,0)$.

written as

$$\rho = \frac{1}{4}\mathbb{I}_4 + \frac{1}{4}\sum_{i=1}^{3}(a_i\sigma_i \otimes \mathbb{I}_2 + b_i\mathbb{I}_2 \otimes \sigma_i) + \frac{1}{4}\sum_{i,j=1}^{3} c_{ij}\sigma_i \otimes \sigma_j, \tag{31}$$

where $\mathbf{a}$ and $\mathbf{b}$ are the Bloch vectors of the marginals, i.e., of $\rho_1 = \mathrm{Tr}_2(\rho)$ and $\rho_2 = \mathrm{Tr}_1(\rho)$, respectively. The action of a unitary transformation on ρ corresponds to the action of a real orthogonal transfer matrix T_2 on $\mathbf{n}_2$. Let us now derive the transfer matrix for common and independent environments.

1. Common environment

In the case of a common environment, one can easily see that, when the common fluctuator is in the state $s_i = \pm 1$, the two-qubit transfer matrix has the following block-diagonal form:

$$T_2(s_i) = \begin{pmatrix} T_{s_i} & 0 & 0 \\ 0 & T_{s_i} & 0 \\ 0 & 0 & T_{s_i} \otimes T_{s_i} \end{pmatrix}, \tag{32}$$

where T_{s_i} was defined in Eq. (20). If we extend the derivation done in Subsection III B for a single qubit, we obtain the following 30×30 matrix:

$$P_2^{\mathrm{CE}} = (\gamma\mathbb{I}_2 - \gamma\sigma_1) \otimes \mathbb{I}_{15} - 2i(\omega\mathbb{I}_2 \otimes Q_z + \sigma_3 \otimes Q_x), \tag{33}$$

where the Q_is, with $i = x, y, z$, are 15×15 block-diagonal matrices

$$Q_i = \begin{pmatrix} L_i & 0 & 0 \\ 0 & L_i & 0 \\ 0 & 0 & L_i \otimes \mathbb{I}_3 + \mathbb{I}_3 \otimes L_i \end{pmatrix}. \tag{34}$$

The ensemble-averaged transfer matrix for $\mathbf{n}_2$ is then

$$T_2^{\mathrm{CE}} = \langle x_f | \exp(-tP_2) | i_f \rangle, \tag{35}$$

where $|i_f\rangle = |x_f\rangle = \frac{1}{\sqrt{2}}(|+\rangle + |-\rangle)$ and the partial inner product is again done on the two degrees of freedom of the fluctuator. An analytic expression for T_2^{CE} cannot be obtained explicitly because we first need to calculate the exponential of P_2, i.e., diagonalize it. However, the exponentiation can be done easily with arbitrary precision once we substitute numerical values.

2. Independent environments

In the case of independent environments, the transfer matrix is simply

$$T_2^{\mathrm{IE}} = \begin{pmatrix} T & 0 & 0 \\ 0 & T & 0 \\ 0 & 0 & T \otimes T \end{pmatrix}, \tag{36}$$

where T is defined in Eq. (23). The analytic solution for the one- and two-qubit dynamics under RTN noise has been compared to the numerical simulations, showing excellent agreement.

D. Properties of the dynamical map

1. Maximally mixed marginals

Equation (36) shows that the two-qubit transfer matrix in the case of independent environments is block diagonal. The same can be seen for the matrix T_2^{CE}. This means that if the initial block vector has $\mathbf{a} = \mathbf{b} = 0$, i.e., the state has maximally mixed marginals, then they will be left untouched by the dynamics. This allows us to apply Luo analytic formula[52] for quantum discord to the evolved state. Although we do not have an analytic expression for the dynamics in case of other kinds of noise, such as Gaussian noise, we can see that the transfer matrix for an infinitesimal time step is block diagonal as well. Thus, in general, we can restrict to the set of states with maximally mixed marginals and use Luo formula for the evaluation of quantum discord.

Upon restricting our choice of the initial state to Bell-state mixtures, we are also able to picture the trajectory of the system. In view of the spectral decomposition theorem, the matrix C of Eq. (30), if symmetrical, can be diagonalized by means of an orthogonal matrix, to which correspond two local unitary operations on the two qubits.[52] It is straightforward to check that Bell-state mixtures have a symmetric C matrix. One can also see analytically that the transfer matrix for the RTN noise with independent environments, Eq. (36), preserves the symmetric nature of the matrix. The same can be seen numerically for T_2^{CE} and also for Gaussian noise. Since all measures of quantum correlations are invariant under local unitary operations, we can always cast C into its diagonal form and represent the two-qubit states with mixed marginals in a tridimensional space where the coordinates are the eigenvalues of C. In this space, the four Bell states occupy the vertexes of a tetrahedron, as shown in Figs. 3 and 4. In the figures, the octahedron of separable Bell-state mixtures is highlighted. The zero-discord states lie on the axes.

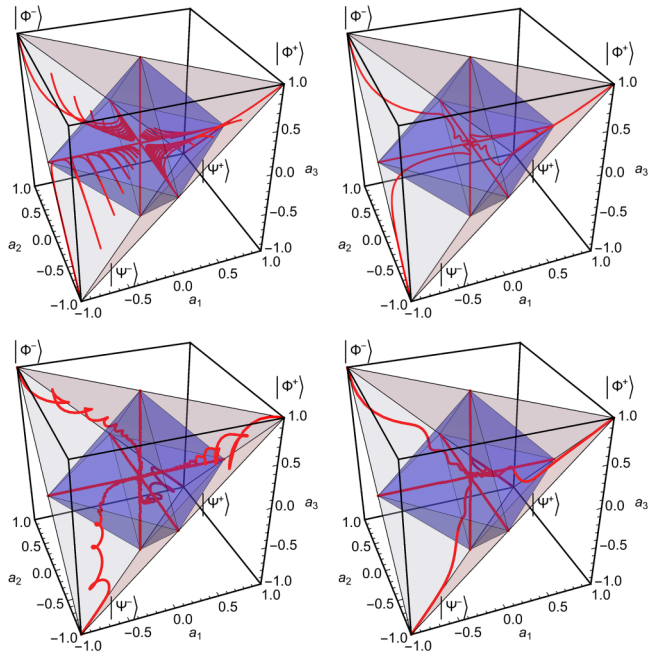

FIG. 3. Trajectories of a two-qubit system in the Bell-state tetrahedron, starting from different initial states, under the influence of RTN (above) and OU noise (below) with $\gamma = 0.1$ (left) and $\gamma = 1$ (right), $\omega = 1$. The dark-blue octahedron is the set of separable states. We can see that the trajectories converge to the state in the origin, i.e., the maximally mixed state $\mathbb{I}/4$. The trajectories, however, get more convoluted for smaller values of γ, and, for the RTN noise, one can see that they get in and out of the set of separable states, and this corresponds to the sudden death and rebirth of entanglement.

2. Stable states of the dynamics

For the single-qubit RTN map, the only fixed point is the maximally mixed state (with the Bloch vector $\vec{0}$). This can be seen from the fact that none of the eigenvalues of P is zero and thus the transfer matrix does not have one as eigenvalue. Figure 2 shows two trajectories, both converging to the center of the Bloch sphere. The same generalizes immediately to the two-qubit case with independent environments. The stable state is the maximally mixed state $\rho = \mathbb{I}/4$. In the CE case, the P_2 matrix has the eigenvalue zero. The corresponding eigenvector is the generalized Bloch vector with $\mathbf{a} = \mathbf{b} = 0$

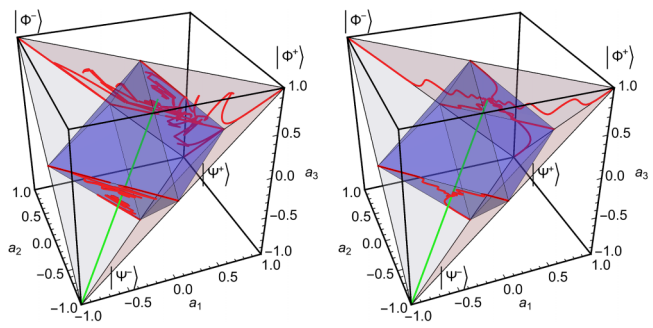

FIG. 4. Trajectories of the system in the Bell-state tetrahedron when the qubits interact with a RTN, common environment, $\omega = 1$ for $\gamma = 1/2$ (left) and $\gamma = 5$ (right). The solid green line denotes the set of Werner states, which are the only stable states. The trajectories lie on planes that are orthogonal to the green line. Similar plots are obtained for Gaussian noise.

and $(c_{ij}) = \mathbb{I}_3$. This means that all Werner states of the form

$$\rho_p^W = p|\Phi^-\rangle\langle\Phi^-| + (1-p)\mathbb{I}/4, \qquad p \in [0,1], \tag{37}$$

where $|\Phi^-\rangle = 1/\sqrt{2}(|01\rangle - |10\rangle)$ is the Bell singlet state, are stationary states of the dynamics. This can also be seen because they satisfy the relation $\rho_p^W = (U \otimes U)\rho_p^W(U^\dagger \otimes U^\dagger)$ for every local unitary U and the CPT map induced by a common reservoir is a convex combination of unitary maps of the form $U \otimes U$. Being the zero eigenvalue of P_2 non-degenerate, these are the only stable states of the map. The same results are seen numerically for the Gaussian noise, although in this case we do not have an analytic expression for the transfer matrix.

IV. COMPARISON OF THE DYNAMICS IN THE PRESENCE OF GAUSSIAN AND NON-GAUSSIAN NOISE

In this section, we compare the dynamics induced by Gaussian and non-Gaussian RTN noise and discuss their effects on the decoherence of quantum correlations of a two-qubit system. We start by noticing that the spectrum of the noise (or equivalently, its autocorrelation function) is in general not enough to describe the effect of the noise on the qubit, i.e., the dynamics of the qubit under the influence of OU noise and RTN with the same spectral width and with the same coupling may be, in general, rather different.

In Fig. 5 we show how the negativity and quantum discord evolve in time for the two models of noise for different values of the spectral width γ. The initial state is a pure Bell state. For both noises, we can identify two working regimes. In the first one, for small γ (slow noise), quantum correlations oscillate heavily and there are sudden deaths and rebirths of entanglement. This can be seen in the top left diagram of Fig. 3: the trajectory of the system repeatedly goes in and out the octahedron of separable states. The frequency of oscillations depends on ω and is doubled if the two qubits are affected by a common environment. In the second regime (large γ, i.e., fast noise), the correlations decay to zero, with sudden death of entanglement and with oscillations. The time constant of the decay is roughly inversely proportional to γ, i.e., the decay is slower for very fast noise. In the common-environment case, we notice that the discord does not vanish in time. The reason is that the stable state of the dynamics does not lie in the set of states with zero discord (cf. Fig. 4).

In order to compare quantitatively the dynamics of the system in the presence of the two kind of noise, we introduce the fidelity complement

$$\tilde{\mathcal{F}}(t) = 1 - \mathcal{F}(\rho_{\rm OU}(t), \rho_{\rm RTN}(t)), \tag{38}$$

where

$$\mathcal{F}(\rho_{\rm OU}(t), \rho_{\rm RTN}(t)) = {\rm Tr}\left[\sqrt{\sqrt{\rho_{\rm OU}(t)}\rho_{\rm RTN}(t)\sqrt{\rho_{\rm OU}(t)}}\right] \tag{39}$$

is the quantum fidelity[64] between the state of a single qubit affected by RTN and the state of a qubit affected by OU, assuming that the two kinds of noise have the same coupling and spectral width. When this quantity is zero, the two states are identical. In the left panel of Fig. 6, we show the fidelity complement as a function of time. We can see that $\tilde{\mathcal{F}}(t)$ is not vanishing when the two noises have the same autocorrelation time. However, upon changing γ, we can reduce its value of three orders of magnitude.

Notice that there is an initial regime in which the fidelity complement increases and a second regime in which it vanishes, as the system tends to its asymptotic maximally mixed state, and hence there is a global maximum of the fidelity complement, $\max[\tilde{\mathcal{F}}(t)]$, which depends on $\gamma_{\rm RTN}$. This maximum can be used as a figure of merit of how good the simulation of Gaussian noise is. In the right panel, we show that $\max[\tilde{\mathcal{F}}(t)]$ can be driven very close to zero by a suitable choice of the parameter γ. It should be noticed, however, that the optimal value of the parameter does depend

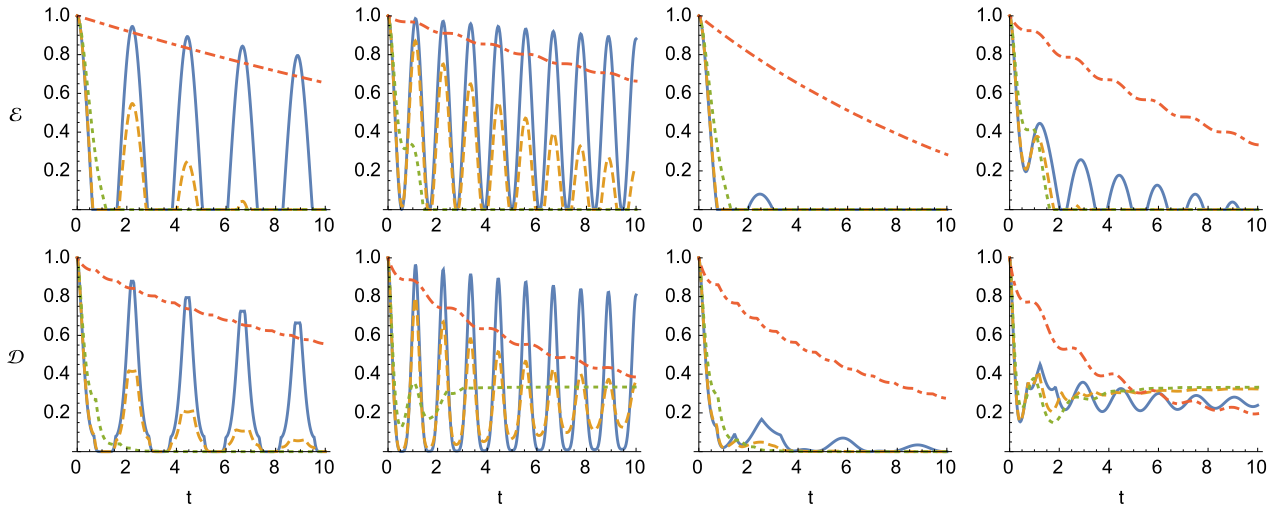

FIG. 5. Negativity $\mathcal{E}$ (above) and quantum discord $\mathcal{D}$ (below) as functions of time for a two-qubit system initially prepared in the Bell state $|\Psi^+\rangle = 1/\sqrt{2}(|00\rangle + |11\rangle)$ subject to (a) RTN and (b) OU noise, with independent (left) and common (right) environment ($\omega = 1$). The blue solid line is for $\gamma = 10^{-2}$, the yellow dashed one is for $\gamma = 10^{-1}$, the dotted green is for $\gamma = 1$ and the orange dot-dashed line for $\gamma = 100$. For both noises, for smaller values of γ, quantum correlations oscillate heavily, with sudden deaths and rebirths of entanglement. The effect is more evident for the RTN. The frequency of oscillations doubles in the common-environment case. For higher values of γ, the correlations decay, possibly with small oscillations, and entanglement dies suddenly.

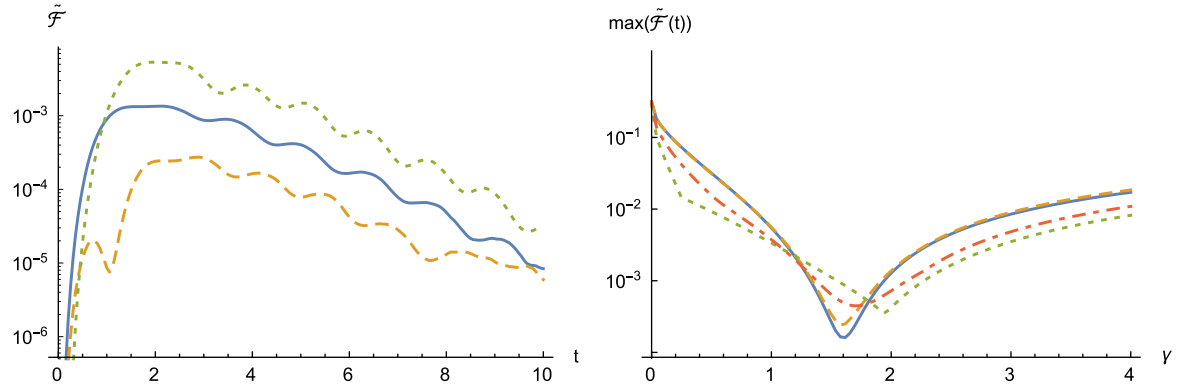

FIG. 6. Left panel: Logarithm of the fidelity complement $\tilde{\mathcal{F}}(t)$ between the state of a qubit ($\omega = 1$) affected by OU noise (with spectral width $\gamma_{\rm OU} = 1$) and RTN as a function of (rescaled) time, for different values of $\gamma_{\rm RTN}$: $\gamma_{\rm RTN} = 1$ (solid blue), $\gamma_{\rm RTN} = 1.5$ (dashed orange), $\gamma_{\rm RTN} = 2$ (dotted green). The qubit is initially prepared in the state $\mathbf{n} = (1, 0, 0)$. We notice that for $\gamma_{\rm RTN} = 1$, i.e., when the two noises have the same spectrum, the dynamics is different. By tuning $\gamma_{\rm RTN}$, the fidelity between the evolved states in the two scenarios may be increased by two orders of magnitude. Right panel: the maximum of the fidelity complement $\tilde{\mathcal{F}}(t)$ as a function of $\gamma_{\rm RTN}$ for $\gamma_{\rm OU} = 1$, initial state set to $\mathbf{n} = (1, 0, 0)$ (solid blue), $\mathbf{n} = (0, 1, 0)$ (dashed yellow), $\mathbf{n} = (0, 0, 1)$ (dotted green), and $\mathbf{n} = (1, 0, 1)/\sqrt{2}$ (dot-dashed orange). We can see that the quality of the simulation depends heavily on the initial state but that by a suitable choice of $\gamma_{\rm RTN}$ we can obtain a fidelity which is above 0.999 throughout the evolution of the qubit.

on the frequency of the qubit, on the parameters of the OU noise and also on the initial state of the qubit, as it is apparent upon looking at the right panel of Fig. 6. We thus conclude that the effects of non-Gaussian noise on qubits cannot be trivially mapped to that of Gaussian noise and vice versa, as that would require that the optimal value of the parameter be independent of the initial state of the qubit(s). This means that the spectrum alone is not enough to characterize the effect of the noise on the qubit systems. On the other hand, the effect of the two noises is qualitatively similar and the dynamics under the effect of one kind of noise may be quantitatively *simulated* with high (quantum) fidelity with the other kind of noise by suitably tuning the parameters.

V. COMPARISON OF NON-MARKOVIANITY MEASURES

In this section, we evaluate the trace-distance-based BLP measure and the entanglement-based RHP measure for the single-qubit map with RTN noise. As a comparison, we recall that the dephasing map with RTN noise[28] is Markovian in the regime of fast noise, i.e., when $\gamma > 2$, while it is non-Markovian in the other regime (slow noise).

For the BLP measure, our numerical results show that the pair of optimal states lies on the equator of the Bloch sphere (i.e., $n_z = 0$), independently on the parameters of the noise. A numerical optimization over the azimuth angle is still in order for computing the measure. The optimal angle depends on the two parameters γ and ω and the dependence is sometimes not smooth. We found that the two measures are in disagreement, i.e., the BLP measure is always non-zero and is vanishing for $\gamma \to \infty$, whereas the RHP measure is vanishing for γ greater than a certain threshold. This is shown in Fig. 7, where the two measures are calculated for a range of values of the switching rate γ and for different values of ω. From Fig. 7 we can see that both measures depend approximately on $1/\gamma$ at small γ. While the RHP measure suddenly goes to zero for γ above a certain threshold value, which depends on ω, the BLP measure only vanishes asymptotically. The BLP measure appears to be independent of ω at small values of γ. We recall

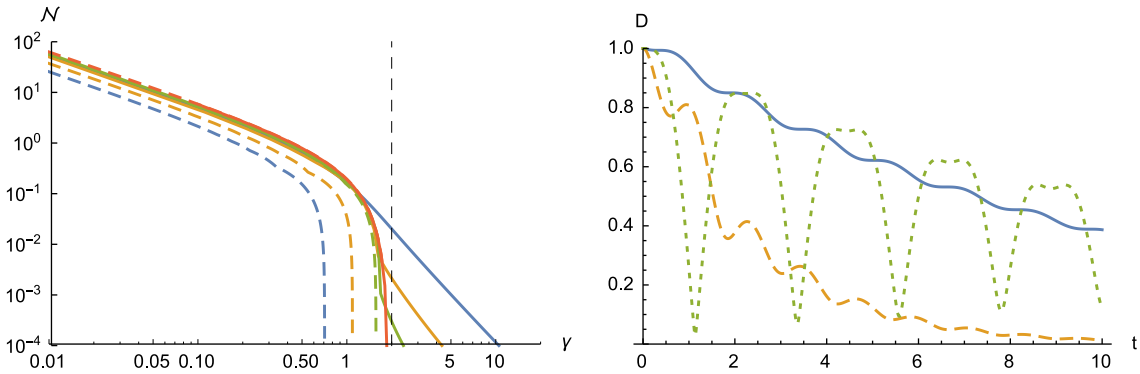

FIG. 7. Left panel: Log-log plot of the non-Markovianity measures $\mathcal{N}_{\rm BLP}$ (solid) and $\mathcal{N}_{\rm RHP}$ (dashed) as functions of the spectral width γ for a qubit subjected to RTN noise, for $\omega = 1$ (blue), $\omega = (2\sqrt{2})^{-1}$ (yellow), $\omega = 0.1$ (green), and $\omega = 0.01$ (orange). The two measures decrease monotonically for increasing γ. There is a threshold value for γ (that depends on ω) above which the RHP measure is zero. The BLP measure, instead, is always non-zero and vanishes for $\gamma \to \infty$, i.e., when $K(t - t') \sim \delta(t - t')$. For small γ, both measures are proportional to $1/\gamma$. For small ω (orange line), we recover the results obtained for the dephasing, with both measures vanishing at $\gamma = 2$ (vertical dashed line). Right panel: Trace distance D between the pairs of states that maximize Eq. (17) as a function of time for $\omega = 1$ and $\gamma = 0.1$ (dotted green), $\gamma = 1$ (dashed orange), $\gamma = 10$ (solid blue). We see that the trace distance oscillates in time: in the intervals in which it increases the map is not divisible. The oscillations get smaller for higher γ: they are barely noticeable in the plot for $\gamma = 10$.

that the two measures only pose a sufficient condition for the dynamical map to be non-divisible, i.e., non-Markovian. The RHP measure fails to capture the non-Markovian behavior of the map because the trajectory quickly enters the set of separable states, as one can see from Fig. 3. On the other hand, the BLP measure is always non-zero, meaning that the map is non-Markovian, unless we let $\omega \to 0$. In this case, we approach the dephasing limit, and the BLP and RHP measures coincide and vanish at $\gamma = 2$.[28] This is shown in the left panel of Fig. 7 for $\omega = 0.01$ (green line). For non-vanishing ω, the non-Markovianity measure vanishes for high values of γ, as one can expect, since the stochastic process that models the noise tends to the Markovian limit, i.e., when $K(t-t') \sim \delta(t-t')$.

In the right panel of Fig. 7, we show, for different values of γ, the behavior of the trace distance $D(t)$ between the pair of states that maximize the integral in Eq. (17). For smaller values of γ, the oscillations are very pronounced. When γ increases, the oscillations become less appreciable ($D(t)$ seems to decay monotonically in the plot for $\gamma = 10$, solid blue line), but derivative of the trace distance is always positive in the first oscillation.

Given the need to optimize over an angle, and the need to reach very long evolution times in order to capture all the oscillations in the trace distance, evaluating the BLP measure for the Gaussian noise is practically unfeasible. However, initial pairs of states can be found for which the trace distance do not decay monotonically for a very wide range of values of γ, and this allows us to conclude that also Gaussian transverse noise with a Lorentzian spectrum induces non-Markovian quantum dynamics on qubits.

VI. CONCLUSIONS

In this paper, we have addressed the dynamics of open single- and two-qubit systems evolving in a classical fluctuating environment described either by Gaussian or non-Gaussian transverse noise, i.e., characterized by a noise spectrum with typical frequencies that are close to the characteristic frequency of the qubit(s). In the two-qubit case, we have considered both the interactions with separate and common environments.

We have analyzed in detail the properties of the quantum map and the dynamics of quantum correlations, also comparing the effects of the two kinds of noise and discussing the stable states of the dynamics.

Upon studying in detail the evolution of an initially maximally entangled state we have identified, for both kinds of noise, two different working regimes. In the first one, when the spectral width of the noise γ is small, quantum correlations oscillate heavily and there are sudden deaths and rebirths of entanglement. The frequency of oscillations depends on ω and is doubled if the two qubits are affected by a common environment. In the second regime, the correlations decay to zero, with sudden death of entanglement and with oscillations. The time constant of the decay is roughly inversely proportional to γ, i.e., the decay is slower for very fast noise. In the common-environment case, the discord does not vanish in time. The reason is that the stable state of the dynamics does not lie in the set of states with zero discord.

Our results indicate that non-Gaussian noise leads to peculiar features that are not present in the Gaussian noise case, in particular, in the slow-noise regime; however, there are regions of the parameter space in which the two noises produce very similar effects on the dynamics of the qubit. This means that while in general the spectrum alone is not enough to characterize the effect of the noise, the dynamics under the effect of one kind of noise may be *simulated* with high quantum fidelity with the other kind of noise by suitably tuning the parameters. This correspondence may in turn be exploited to obtain analytic or semi-analytic results for otherwise intractable kind of (Gaussian) spectrum.

Finally, we have shown that the quantum map is always non-Markovian (contrarily to what happens for a dephasing dynamics in the presence of the same kind of noise) and we quantified the non-Markovianity with the BLP measure for the RTN. We also highlighted the discrepancy between the BLP measure and the RHP measure based on entanglement, which fails to capture the non-Markovianity of the dynamical map for a region of the parameters.

ACKNOWLEDGMENTS

The authors thank C. Benedetti for useful discussions. This work has been supported by EU through the Collaborative Project QuProCS (Grant Agreement No. 641277) and by UniMI through the H2020 Transition Grant No. 15-6-3008000-625.

APPENDIX: TRANSFER MATRIX ELEMENTS

Here, we write explicitly the nonzero elements of the 3×3 transfer matrix T of Eq. (23). Here, μ_i and η_i are the solutions of Eqs. (25) and (26)

$$T_{11} = \frac{e^{\mu_2 t}\left[\mu_1\mu_3\left(1-2\omega^2\right) - 2\omega^2\left(2\gamma^2+\gamma\mu_2-4\omega^2\right)\right]}{4\left[1-\omega^2\left(2\gamma^2+\omega^2\right)\right] + 2\gamma\mu_2\left(1-6\omega^2\right) + \mu_2^2\left(1-5\omega^2\right)} + \frac{e^{\mu_3 t}\left[4-4\omega^2\left(\gamma^2+1\right) + 2\gamma\mu_3\left(1-3\omega^2\right) + \mu_3^2\left(1-2\omega^2\right)\right]}{4\left[1-\omega^2\left(2\gamma^2+\omega^2\right)\right] + 2\gamma\mu_3\left(1-6\omega^2\right) + \mu_3^2\left(1-5\omega^2\right)} + \frac{e^{\mu_1 t}\left\{2\gamma\mu_3\omega^2 + \mu_2\left[2\gamma\omega^2 + \mu_3\left(1-2\omega^2\right)\right] + 8\omega^4\right\}}{4\left[1-\omega^2\left(2\gamma^2+\omega^2\right)\right] + 2\gamma\mu_1\left(1-6\omega^2\right) + \mu_1^2\left(1-5\omega^2\right)}, \tag{A1}$$

$$T_{12} = -T_{21} = \frac{\omega e^{\mu_2 t}\left[4\omega^2(3\gamma+\mu_2) - \gamma\mu_1\mu_3\right]}{4\left[1-\omega^2(2\gamma^2+\omega^2)\right] + 2\gamma\mu_2(1-6\omega^2) + \mu_2^2(1-5\omega^2)} + \frac{\omega e^{\mu_1 t}\left[4\omega^2(\mu_3-\gamma) + \mu_2(\gamma\mu_3+4\omega^2)\right]}{8\gamma^2\omega^2 - 4 - 2\gamma\mu_1(1-6\omega^2) - \mu_1^2(1-5\omega^2) + 4\omega^4} + \frac{\omega e^{\mu_3 t}\left[\mu_3(2\gamma^2+\gamma\mu_3-4\omega^2) + 4\gamma(1-2\omega^2)\right]}{8\gamma^2\omega^2 - 4 - 2\gamma\mu_3(1-6\omega^2) - \mu_3^2(1-5\omega^2) + 4\omega^4}, \tag{A2}$$

$$T_{22} = 2\gamma\omega^2\left\{\frac{e^{\mu_1 t}\left[\mu_2(\gamma-\mu_3) + \gamma\mu_3 + 4(1+\omega^2)\right]}{\gamma\left\{4\left[1-\omega^2(2\gamma^2+\omega^2)\right] + 2\gamma\mu_1(1-6\omega^2) + \mu_1^2(1-5\omega^2)\right\}} + \frac{e^{\mu_2 t}\left(2\gamma^2+\gamma\mu_2-4+\mu_1\mu_3-4\omega^2\right)}{\gamma\left[8\gamma^2\omega^2 - 4 - 2\gamma\mu_2(1-6\omega^2) - \mu_2^2(1-5\omega^2) + 4\omega^4\right]} - \frac{(2\gamma+\mu_3)\,e^{\mu_3 t}}{4\left[1+2\omega^2(1-\gamma^2)+\omega^4\right] + 2\gamma\mu_3(1-2\omega^2) + \mu_3^2(1+\omega^2)}\right\}, \tag{A3}$$

$$T_{33} = 2\omega^2\left\{\frac{(81-\eta_1\eta_3)\,e^{\eta_2 t}}{8\left[1-\omega^2(\gamma^2+\omega^2)\right] + 4\gamma\eta_2(1-4\omega^2) + 2\eta_2^2(1-5\omega^2)} + \frac{(8-\eta_2\eta_3)\,e^{\eta_1 t}}{8\left[1-\omega^2(\gamma^2+\omega^2)\right] + 4\gamma\eta_1(1-4\omega^2) + 2\eta_1^2(1-5\omega^2)} + \frac{e^{\eta_3 t}\left[4\gamma\eta_3 + 4\left(\gamma^2-1+\omega^2\right) + \eta_3^2\right]}{8\left(\gamma^2\omega^2 - 1 + \omega^4\right) - 2\eta_3\left[2\gamma(1-4\omega^2) + \eta_3(1-5\omega^2)\right]}\right\}. \tag{A4}$$

[1]Y. Yan and R. Xu, Annu. Rev. Phys. Chem. **56**, 187 (2005).
[2]V. Privman, J. Stat. Phys. **110**, 957 (2003).
[3]A. J. Leggett, S. Chakravarty, A. T. Dorsey, M. P. A. Fisher, A. Garg, and W. Zwerger, Rev. Mod. Phys. **59**, 1 (1987).
[4]B. D. Laikhtman, Phys. Rev. B **31**, 490 (1985).
[5]N. Wu and Y. Zhao, J. Chem. Phys. **139**, 054118 (2013).
[6]D. Segal, J. Chem. Phys. **140**, 164110 (2014).
[7]P. W. Anderson and P. R. Weiss, Rev. Mod. Phys. **25**, 269 (1953).
[8]J. R. Klauder and P. W. Anderson, Phys. Rev. **125**, 912 (1962).
[9]R. Xu, Y. Mo, P. Cui, S. Lin, and Y. Yan, Prog. Theor. Chem. Phys. **12**, 7–40 (2003).
[10]E. Paladino, M. Y. Galperin, G. Falci, and L. B. Altshuler, Rev. Mod. Phys. **86**, 361 (2014).
[11]E. Paladino, L. Faoro, G. Falci, and R. Fazio, Phys. Rev. Lett. **88**, 228304 (2002).
[12]Y. M. Galperin, B. L. Altshuler, J. Bergli, and D. V. Shantsev, Phys. Rev. Lett. **96**, 097009 (2006).
[13]G. Ramon, Phys. Rev. B **92**, 155422 (2015).
[14]O. Astafiev, Y. A. Pashkin, Y. Nakamura, T. Yamamoto, and J. S. Tsai, Phys. Rev. Lett. **93**, 267007 (2004).
[15]D. Lacroix, Phys. Rev. E **77**, 041126 (2008).
[16]J. Helm and W. T. Strunz, Phys. Rev. A **80**, 042108 (2009).
[17]J. Helm, W. T. Strunz, S. Rietzler, and L. E. Würflinger, Phys. Rev. A **83**, 042103 (2011).
[18]D. Crow and R. Joynt, Phys. Rev. A **89**, 042123 (2014).
[19]W. M. Witzel, K. Young, and S. Das Sarma, Phys. Rev. B **90**, 115431 (2014).
[20]O.-P. Saira, V. Bergholm, T. Ojanen, and M. Möttönen, Phys. Rev. A **75**, 012308 (2007).
[21]J. Shao, J. Chem. Phys. **120**, 5053 (2004).
[22]M. A. C. Rossi, C. Benedetti, and M. G. A. Paris, Int. J. Quantum Inf. **12**, 1560003 (2014).
[23]T. Yu and J. H. Eberly, Opt. Commun. **264**, 393 (2006).
[24]K. Wódkiewicz, B. W. Shore, and J. H. Eberly, Phys. Rev. A **30**, 2390 (1984).
[25]J. Bergli, Y. M. Galperin, and B. L. Altshuler, New J. Phys. **11**, 025002 (2009).
[26]C. Benedetti, F. Buscemi, P. Bordone, and M. G. A. Paris, Phys. Rev. A **87**, 052328 (2013).
[27]L. Mazzola, J. Piilo, and S. Maniscalco, Int. J. Quantum Inf. **9**, 981 (2011).
[28]C. Benedetti, M. G. A. Paris, and S. Maniscalco, Phys. Rev. A **89**, 012114 (2014).
[29]C. Benedetti, F. Buscemi, P. Bordone, and M. G. A. Paris, Phys. Rev. A **89**, 032114 (2014).
[30]C. Benedetti and M. G. A. Paris, Phys. Lett. A **378**, 2495 (2014).
[31]G. A. Álvarez and D. Suter, Phys. Rev. Lett. **107**, 230501 (2011).
[32]A. Zwick, G. A. Alvarez, and G. Kurizki, "Maximizing information on the environment by dynamically controlled qubit probes," Phys. Rev. Appl. (to be published).
[33]M. A. C. Rossi and M. G. A. Paris, Phys. Rev. A **92**, 010302 (2015).
[34]P. Szańkowski, M. Trippenbach, Ł. Cywiński, and Y. B. Band, Quantum Inf. Process. **14**, 3367 (2015).
[35]P. Szańkowski, M. Trippenbach, and Ł. Cywiński, e-print arXiv:1507.03897 [cond-mat.mes-hall] (2015).
[36]A. Shnirman, Y. Makhlin, and G. Schön, Phys. Scr. **T102**, 147 (2002).
[37]J. Schriefl, Y. Makhlin, A. Shnirman, and G. Schön, New J. Phys. **8**, 1 (2006).
[38]J. I. Vestgården, J. Bergli, and Y. M. Galperin, Phys. Rev. B **77**, 014514 (2008).
[39]F. C. Lombardo and P. I. Villar, Phys. Rev. A **89**, 012110 (2014).
[40]M. Crescimanno, Ann. Phys. (N. Y.) **223**, 229 (1993).
[41]X. Zhu, S. Saito, A. Kemp, K. Kakuyanagi, S.-i. Karimoto, H. Nakano, W. J. Munro, Y. Tokura, M. S. Everitt, K. Nemoto, M. Kasu, N. Mizuochi, and K. Semba, Nature **478**, 221 (2011).
[42]Y. Matsuzaki and H. Nakano, Phys. Rev. B **86**, 184501 (2012).
[43]J. Li, M. P. Silveri, K. S. Kumar, J.-M. Pirkkalainen, A. Vepsäläinen, W. C. Chien, J. Tuorila, M. A. Sillanpää, P. J. Hakonen, E. V. Thuneberg, and G. S. Paraoanu, Nat. Commun. **4**, 1420 (2013).
[44]T. Hayashi, T. Fujisawa, H. D. Cheong, Y. H. Jeong, and Y. Hirayama, Phys. Rev. Lett. **91**, 226804 (2003).
[45]H. Risken, L. Schoendorff, and K. Vogel, Phys. Rev. A **42**, 4562 (1990).
[46]M. Aihara, H. M. Sevian, and J. L. Skinner, Phys. Rev. A **41**, 6596 (1990).
[47]G. De Chiara and G. M. Palma, Phys. Rev. Lett. **91**, 090404 (2003).
[48]A. Fiasconaro and B. Spagnolo, Phys. Rev. E **80**, 041110 (2009).
[49]C. Benedetti and M. G. A. Paris, Int. J. Quantum Inf. **12**, 6 (2014).
[50]G. Vidal and R. F. Werner, Phys. Rev. A **65**, 032314 (2002).
[51]H. Ollivier and W. H. Zurek, Phys. Rev. Lett. **88**, 017901 (2001).
[52]S. Luo, Phys. Rev. A **77**, 042303 (2008).
[53]A. Rivas, S. F. Huelga, and M. B. Plenio, Phys. Rev. Lett. **105**, 050403 (2010).
[54]H.-P. Breuer, E.-M. Laine, and J. Piilo, Phys. Rev. Lett. **103**, 210401 (2009).
[55]S. Wißmann, A. Karlsson, E.-M. Laine, J. Piilo, and H.-P. Breuer, Phys. Rev. A **86**, 062108 (2012).
[56]W. Magnus, Commun. Pure Appl. Math. **7**, 649 (1954).
[57]J. Budimir and J. Skinner, J. Stat. Phys. **49**, 1029 (1987).
[58]R. Der and W. Schumacher, Z. Phys. B **83**, 295 (1991).
[59]L. Andreozzi, C. Donati, M. Giordano, and D. Leporini, Phys. Rev. A **46**, 6222 (1992).
[60]B. Cheng, Q.-H. Wang, and R. Joynt, Phys. Rev. A **78**, 022313 (2008).
[61]I. A. Goychuk, Phys. Rev. E **51**, 6267 (1995).
[62]I. Goychuk and P. Hänggi, Chem. Phys. **324**, 160 (2006).
[63]P. Bordone, F. Buscemi, and C. Benedetti, Fluctuation Noise Lett. **11**, 1242003 (2012).
[64]M. A. Nielsen and I. L. Chuang, *Quantum Computation and Quantum Information* (Cambridge University Press, 2010).